A Journal of the Gesellschaft Deutscher Chemiker

Angewandte International Edition GDCh Chemie

www.angewandte.org

Accepted Article

Title: Chemical Vapor Deposition of Phase-Pure Uranium Dioxide Thin Films from Uranium(IV) Amidate Precursors.

Authors: Mark Straub, Jennifer Leduc, Michael Frank, Aida Raauf, Trevor Lohrey, Stefan Minasian, John Arnold, and Sanjay Mathur

To be cited as: *Angew. Chem. Int. Ed.* 10.1002/anie.201901924
Angew. Chem. 10.1002/ange.201901924

Link to VoR: http://dx.doi.org/10.1002/anie.201901924
http://dx.doi.org/10.1002/ange.201901924

WILEY-VCH

10.1002/anie.201901924

WILEY-VCH

Chemical Vapor Deposition of Phase-Pure Uranium Dioxide Thin Films from Uranium(IV) Amidate Precursors

Mark Straub[a,b], Jennifer Leduc[c], Michael Frank[c], Aida Raauf[c], Trevor Lohrey[a,b], Stefan Minasian,[b] Sanjay Mathur*[c], and John Arnold*[a,b]

Abstract: Homoleptic uranium(IV) amidate complexes have been synthesized and applied as single-source molecular precursors for chemical vapor deposition of UO_2 thin films. These precursors decompose by alkene elimination to give highly crystalline, phase-pure UO_2 films with an unusual branched heterostructure.

The efficiency and safety profiles of nuclear reactors are heavily impacted by the surface chemistry of the fuel materials used in the reactor core.[1] Defect formation and void swelling in UO_2 fuel pellets dramatically reduce the lifetime and energy output of these materials, but direct study of the surface oxidation processes that cause these defects can be challenging due to the chemical complexity and extreme radioactivity of spent fuels.[1–3] Due to their large active surface areas, phase-pure UO_2 thin films can serve as excellent model systems for the chemical and physical changes that occur at the grain boundaries of bulk UO_2 fuel pellets. Uranium oxide thin films have been fabricated using both solution[4–6] and sputtering[7–10] methods; however, achieving stoichiometric control in the resulting films has been challenging due to the wide array of accessible uranium oxide phases and the facile interconversion of these phases at grain boundaries.[5,11] Consequently, many published studies on uranium oxide have been performed using materials with a varying degree of amorphous or polycrystalline character.[12] McClesky and coworkers have used an innovative polymer-assisted deposition technique from $UO_2(NO_3)_2$ precursors to produce UO_2 and U_3O_8 thin films; epitaxial matching of the desired uranium oxide phase to the substrate, followed by annealing at 1000 °C, resulted in phase-pure films.[12,13] Chemical vapor deposition (CVD) is an additional promising route, with the added benefit that direct synthesis of uranium oxide films from a single-source molecular precursor could facilitate enhanced tunability of the growth process through rational control of the decomposition mechanism and rate.[14] However, the preparation of phase-pure thin films in a CVD process can be challenging, as the precursors must be both sufficiently volatile and decompose cleanly by a single mechanism to minimize the formation of side products.[15]

The last few decades have yielded an enormous amount of research into volatile transition metal and lanthanide complexes, which are used as molecular precursors for CVD of metal oxide, nitride, sulfide, and carbide thin films.[14,16–22] In contrast to the myriad quantity of CVD precursors that have been described for these metals, only a small handful of uranium oxide CVD precursors have ever been reported. The first gas-phase synthesis of uranium oxide thin films was accomplished by heating a uranyl β-diketonate precursor above 400 °C in the presence of O_2 or H_2O; however, the oxidizing environment of these reactive gases prevented the formation of phase-pure UO_2 films.[23] In a more recent single-source process, films containing a mixture of uranium oxides were synthesized via thermal CVD from fluorinated uranium heteroarylalkenolate precursors.[24] We sought to develop a class of volatile, non-fluorinated precursors with an easily-accessible thermal decomposition pathway to UO_2, thereby minimizing the heat required to form phase-pure UO_2 films. Based on previous research in our group[25] and promising results from related transition metal systems,[26–28] we turned to uranium amidate complexes to meet these requirements. Amidate ligand substituents can be readily varied to cover a wide range of steric and electronic properties, enabling control over the geometry, thermal stability, volatility, and decomposition mechanisms of the resulting metal complexes. Using new U^{IV} amidate precursors with a well-defined decomposition mechanism, we synthesized crystalline, phase-pure UO_2 films via CVD.

The amide proligands N-*tert*-butylisobutyramide (H(ITA)) (**1**) and N-*tert*-butylpivalamide (H(TTA)) (**2**) were synthesized according to literature methods[29] and purified by sublimation. Deprotonation of **1** and **2** with $KN(SiMe_3)_2$ in THF generated the corresponding potassium amidates K(ITA) (**3**) and K(TTA) (**4**) in high yield. As we have observed previously in related systems,[25] using these potassium amidates directly for the metalation of uranium led to the formation of undesirable –ate complexes, resulting in poor yields of the anticipated products. This was overcome by adding 18-crown-6 to **3** and **4** to give the crowned potassium amidates K(ITA)(18c6) (**5**) and K(ITA)(18c6) (**6**) in near-quantitative yield *(Scheme 1)*; these ligand salts performed much more favorably for metalation of uranium.

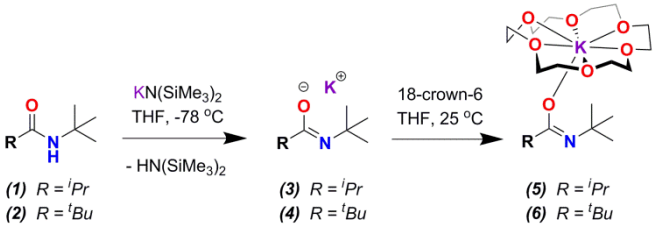

Scheme 1. *Synthesis of the crowned potassium amidates K(ITA)(18c6) (**5**) and K(TTA)(18c6) (**6**).*

[a] M. D. Straub, T. D. Lohrey, Prof. Dr. J. Arnold*
Department of Chemistry, University of California, Berkeley
Berkeley, CA 94720, USA
E-mail: arnold@berkeley.edu
[b] M. D. Straub, T. D. Lohrey, S. G. Minasian, Prof. Dr. J. Arnold*
Heavy Element Chemistry Group, Chemical Sciences Division
Lawrence Berkeley National Lab
Berkeley, CA 94720, USA
[c] J. Leduc, M. Frank, A. Raauf, Prof. Dr. S. Mathur*
Institute of Inorganic Chemistry, University of Cologne
Cologne, Germany 50939

Supporting information for this article is given via a link at the end of the document.

The homoleptic amidate complexes U(ITA)$_4$ (**7**) and U(TTA)$_4$ (**8**) were synthesized by treating UI$_4$(1,4-dioxane)$_2$ with four equivalents of **5** or **6**, respectively. *(Scheme 2)* We also synthesized **7** and **8** via a protonolysis route with [(Me$_3$Si)$_2$N]$_2$U[κ^2-(*C*,*N*)-CH$_2$Si(Me)$_2$N(SiMe$_3$)] and **1** or **2**, but yields were lower using this method. Green crystals of **7** and teal crystals of **8** suitable for X-ray diffraction were grown from Et$_2$O and pentane, respectively.

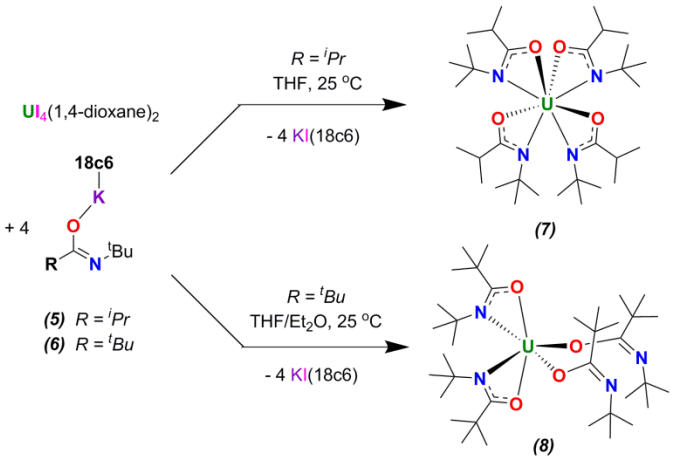

Scheme 2. *Synthesis of U(ITA)$_4$ **(7)** and U(TTA)$_4$ **(8)**.*

Although the proligands **1** and **2** are comparable sterically, we observed different molecular geometries for **7** and **8**. Crystallographic analysis of **7** showed this molecule to be eight-coordinate and D_{2d} symmetric, with all four amidate ligands chelated (κ$_2$-*N,O*) to the uranium center. By comparison, **8** is six-coordinate and C_1 symmetric, with two (κ$_2$-*N,O*) amidate ligands and two (κ$_1$-*O*) amidate ligands bound to the uranium center. This difference in geometry can possibly be attributed to the higher electron donating effect of the *tert*-butyl vs. *iso*-propyl substituents on the amidate backbone, disfavoring electron donation from the lone pairs on all four nitrogen atoms to the uranium center in **8**; however, it is also possible that the larger steric bulk of the C-^{t}Bu substituent contributes to the lower coordination number of **8**.

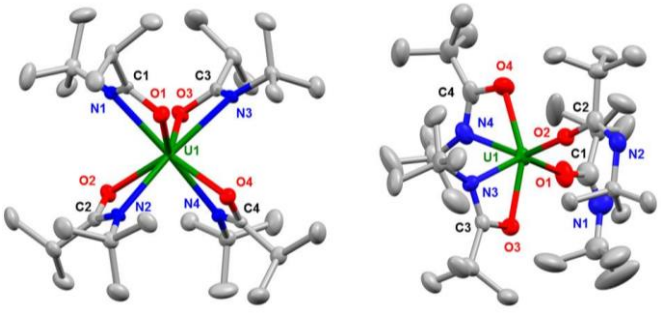

Figure 1. *50% probability thermal ellipsoid view of U(ITA)$_4$ **(7)** (left) and U(TTA)$_4$ **(8)** (right). Hydrogen atoms are omitted for clarity.*

Table 1. *Selected bond lengths in **7** and **8**.*

Atoms	Bond lengths (Å)	
	7	**8**
U1 – O1	2.333(2)	2.123(5)
U1 – O2	2.350(2)	2.135(4)
U1 – O3	2.366(2)	2.284(4)
U1 – O4	2.346(2)	2.296(4)
U1 – N1	2.499(3)	-
U1 – N2	2.507(2)	-
U1 – N3	2.502(2)	2.495(5)
U1 – N4	2.493(3)	2.457(5)
C1 – O1	1.307(4)	1.375(9)
C2 – O2	1.311(3)	1.361(7)
C3 – O3	1.296(4)	1.323(7)
C4 – O4	1.303(4)	1.323(7)
C1 – N1	1.305(4)	1.141(11)
C2 – N2	1.292(4)	1.240(9)
C3 – N3	1.296(4)	1.297(8)
C4 – N4	1.310(4)	1.309(9)

The U-O and U-N bond lengths in **7** are comparable to the analogous U-O and U-N bonds of the chelated amidates in **8** (2.284(4) and 2.296(4) Å for U-O). However, the U-O bonds of the O-bound amidates in **8** are substantially shorter (2.123(5) and 2.135(4) Å), suggesting increased localization of electron density on the oxygen atoms of these ligands when bound κ$_1$-*O*. Providing further support for this claim, the O-bound ligands in **8** also possess longer C-O bonds (1.375(9) and 1.361(7) Å) and shorter C-N bonds (1.141(11) and 1.240(9) Å for C-N) than their chelated counterparts (1.323(7) and 1.323(7) Å for C-O; 1.297(8) and 1.309(9) Å).

The thermal decomposition of the precursors was further investigated using thermogravimetric (TG) analysis (*Figure 2*). Precursor **7** showed an onset of decomposition at 85 °C, while precursor **8** showed an onset of decomposition at 70 °C. The experimentally detected overall weight losses of **7** (65.0%) and **8** (62.7%) are lower than the theoretical values of 66.5% and 68.8% for the formation of UO$_2$, suggesting the potential incorporation of carbon impurities; this mass difference is substantially more prominent for precursor **7** than for precursor **8**. An in-depth discussion on the TG analysis can be found in the supporting information.

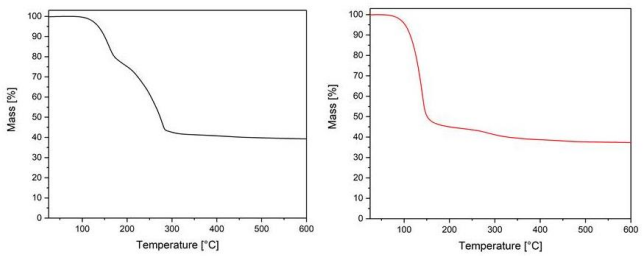

Figure 2. *Thermograms of **7** (left) and **8** (right) collected under nitrogen at a heating rate of 5 °C/min.*

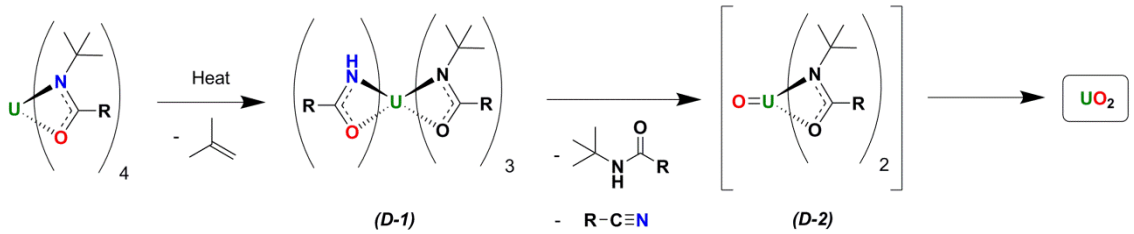

Scheme 3. *Proposed decomposition mechanism of **7** and **8**. Alkene, amide, and nitrile byproducts were observed by NMR; intermediate decomposition products **D-1** and **D-2** are postulated.*

To elucidate the decomposition mechanism of these precursors to uranium oxide, solid samples of **7** and **8** were heated to 300 °C in sealed J-Young tubes under a nitrogen atmosphere. The tubes were then cooled with liquid nitrogen to condense volatile decomposition products, and C_6D_6 was added for NMR analysis. Three main products were visible in the resulting ^{1}H NMR spectra of the decomposed precursors: the amides **1** or **2**, isobutyronitrile (from **7**) or pivalonitrile (from **8**), and isobutylene. A small amount of insoluble black uranium oxide precipitate was also observed. These products are consistent with an alkene elimination mechanism *(Scheme 3)*, as reported previously for related homoleptic Zr(IV) amidates.[26] We also observed slow formation of the same products by heating solutions of **7** and **8** to 150 °C in d_8-toluene over the course of multiple days.

In the first decomposition step, isobutylene elimination from a nitrogen atom generates a hemiamidate intermediate (**D-1**). This hemiamidate then undergoes protonolysis with another amidate ligand to promote the elimination of one equivalent each of amide and nitrile, leaving an oxygen atom bound to the uranium center **(D-2)**. Because this is a low-coordinate system, it is likely that the intermediate **D-2** aggregates prior to elimination of additional ligands. A second iteration of this process yields UO_2 and one more equivalent each of isobutylene, amide, and nitrile.

Complexes **7** and **8** were both tested as UO_2 thin film precursors in a cold wall thermal CVD reactor. We were interested to determine if the oxidation state of the precursors would be retained in the CVD-generated materials to form stoichiometric UO_2 films, as suggested by the thermal decomposition experiments. As the sublimation temperatures and decomposition temperatures at a pressure of 10^{-3} mbar were in very close vicinity (~130 °C for **7**, ~120 °C for **8**), CVD experiments were performed at a pressure of 10^{-6} mbar to favor sublimation of the precursors. In order to ensure a proper precursor flow, the precursor temperatures were set to 160 °C. Since TG analysis displayed a complete decomposition of both precursors at a temperature of 500 °C, substrate temperatures of 500 °C were chosen for both CVD processes. Precursor **7** sublimed without prior decomposition in the precursor flask, and black films were generated during the CVD process. In contrast, the deposition process using complex **8** was not successful; we postulate this may be due to the weakly bound κ_1-*O* coordinated ligands and thus thermal instability of the precursor.

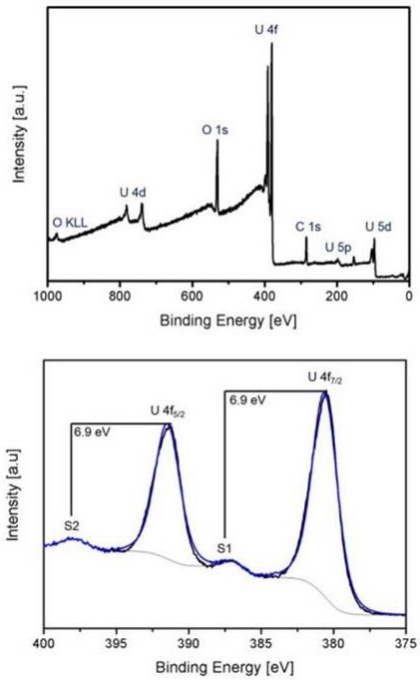

Figure 3. *XPS survey spectrum (top) and high-resolution U 4f XPS spectrum (bottom) of crystalline UO_2 films prepared via CVD using **7**.*

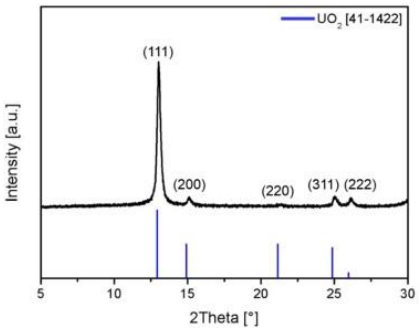

Figure 4. *Powder XRD pattern of the film deposited using **7** at a precursor temperature of 160 °C and a substrate temperature of 500 °C.*

Following the deposition process, the films were characterized without an additional annealing step to determine if UO_2 was prepared directly. As shown by XPS (*Figure 3*) and XRD (*Figure 4*) analyses, the film surface and the bulk are composed of phase-pure UO_2. This finding is noteworthy given the pronounced tendency of uranium dioxide to exhibit surface oxidation resulting in hyperstoichiometric compositions (O:U > 2:1). The XPS survey spectrum exhibited signals attributable solely to uranium, oxygen and carbon (*Figure 3*, left). The high-resolution U 4f XPS spectrum showed two main signals at 380.4 eV and 391.4 eV, corresponding to the U $4f_{7/2}$ and U $4f_{5/2}$ orbitals, respectively (*Figure 3*, right). The peak positions of the main signals and the satellites (binding energy distance to the main signals of DE_{sat} = 6.9 eV) are consistent with the reported data.[5] The Bragg reflections in the XRD pattern were assigned to cubic fluorite-type UO_2 (*Figure 4*). The peaks at 2θ = 13.0°, 15.0°, 21.2°, 24.9° and 26.0° were indexed to the (111), (200), (220), (311) and (222) planes, respectively. As the diffraction peaks are broadened anisotropically, the crystallite sizes were calculated using the Scherrer equation and amounted to 146 nm, 195 nm and 99 nm for the (111)/(222), (200) and (311) planes, respectively. Whereas the anisotropic broadening suggests the formation of anisotropic crystallite shapes, the predominant intensity of the reflection indexed to the (111) plane hints towards a preferred growth direction that was confirmed by the surface topography (*Figure 5*). Taken together, these results strongly suggest that phase-pure UO_2 films were prepared directly via decomposition of the molecular precursor.

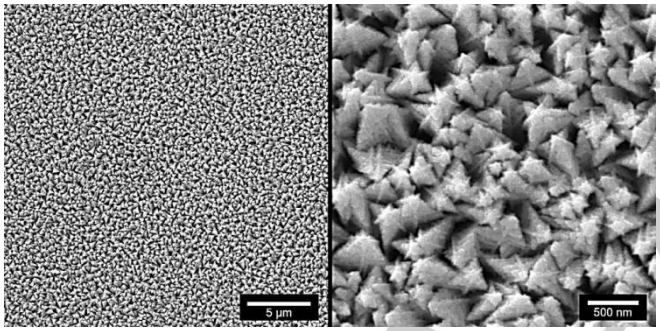

Figure 5. *Top-view SEM images with different magnifications of crystalline UO_2 films, prepared via CVD from precursor **7**.*

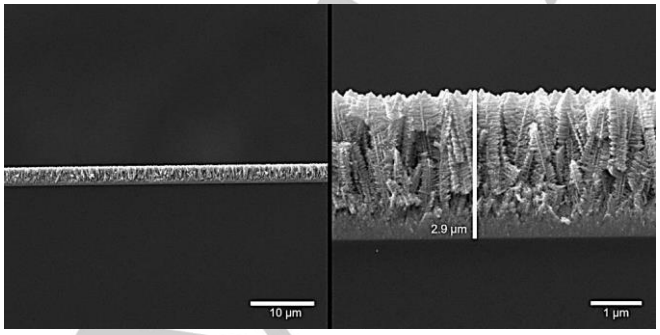

Figure 6. *Side-view SEM images with different magnifications of crystalline UO_2 films, prepared via CVD from precursor **7**. The thickness of these films is 2.9 µm.*

The vapor-deposited UO_2 films exhibited a homogeneous distribution of fir tree-like structures at the surface and good adhesion to the silicon substrate, as depicted in the top-view (*Figure 5*) and side-view (*Figure 6*) SEM images, respectively. The side-view SEM images additionally revealed the formation of a dense layer with a thickness of ~400 nm at the substrate interface, which seamlessly continues into a branch-like structure with a thickness of ~2.5 µm. This change in the microstructure from 2-D to 1-D growth is likely due to the good lattice match between silicon (a = 5.431 Å) and UO_2 (a = 5.471 Å), which facilitates epitaxial growth of UO_2 onto Si up to a thickness of ca. 400 nm. Beyond this thickness, the cubic UO_2 crystals act as seeds for 1-D nanostructures that grow with equal probability in multiple directions, leading to the formation of branch-like structures.

In summary, we have developed an effective single-source route to fabricate crystalline, phase-pure UO_2 films through chemical vapor deposition of U^{IV} amidate molecular precursors, which decompose cleanly via alkene elimination. Small changes in the ligand substituents were seen to affect both the molecular geometry and the decomposition behavior of the precursors, with the 8-coordinate complex **7** performing much more favorably for thin film deposition than the 6-coordinate complex **8**. XRD and XPS measurements confirmed the vapor-deposited uranium oxide films to be stoichiometric UO_2, and SEM images showed good epitaxial growth of the UO_2 layer onto the Si substrate. Above a film thickness of ca. 400 nm, the UO_2 crystals formed fir tree-like structures with isotropic growth of 1-D branches and a large accessible surface area. Given the anisotropic microstructure and high surface area of these films, in conjunction with high charge carrier mobilities in UO_2, we plan to investigate the performance of these films as photoanodes in photoelectrochemical water splitting reactions.

Acknowledgements

This work was supported by the Director, Office of Science, Office of Basic Energy Sciences, Division of Chemical Sciences, Geosciences, and Biosciences Heavy Element Chemistry Program of the U.S. Department of Energy (DOE) at LBNL under Contract No. DE-AC02-05CH11231. The Advanced Light Source (ALS) is supported by the Director, Office of Science, Office of Basic Energy Sciences, of the U.S. Department of Energy under Contract No. DE-AC02-05CH11231. We thank Dr. Simon J. Teat for oversight of our crystallographic studies at the ALS. We also thank M. A. Boreen, N. S. Settineri, and L. M. Moreau for helpful discussions. J.L., M.F., A.R. and S.M. are thankful to the University of Cologne for providing the infrastructural support. J.L. is thankful to Fonds der Chemischen Industrie for a PhD fellowship. A.R. acknowledges the DAAD for a travel grant. The financial support in the framework of the DFG priority programs (SPP 1613; "Fuels Produced Regeneratively Through Light-Driven Water Splitting: Clarification of the Elemental Processes Involved and Prospects for Implementation in Technological Concepts" and SPP 1959 "Manipulation of

matter controlled by electric and magnetic field: Towards novel synthesis and processing routes of inorganic materials") are gratefully acknowledged.

Keywords: Uranium • Inorganic materials • Chemical vapor deposition • Thin films • Actinides

[1] S. J. Zinkle, G. S. Was, *Acta Mater.* **2013**, *61*, 735–758.
[2] S. J. Zinkle, K. A. Terrani, J. C. Gehin, L. J. Ott, L. L. Snead, *J. Nucl. Mater.* **2014**, *448*, 374–379.
[3] K. Nogita, K. Une, *J. Nucl. Mater.* **1997**, *250*, 244–249.
[4] S. R. Qiu, C. Amrhein, M. L. Hunt, R. Pfeffer, B. Yakshinskiy, L. Zhang, T. E. Madey, J. A. Yarmoff, *Appl. Surf. Sci.* **2001**, *181*, 211–224.
[5] H. Idriss, *Surf. Sci. Rep.* **2010**, *65*, 67–109.
[6] T. T. Meek, B. Von Roedern, P. G. Clem, R. J. Hanrahan, *Mater. Lett.* **2005**, *59*, 1085–1088.
[7] T. S. Noggle, J. O. Stiegler, *J. Appl. Phys.* **1960**, *31*, 2199–2208.
[8] Q. Chen, X. Lai, B. Bai, M. Chu, *Appl. Surf. Sci.* **2010**, *256*, 3047–3050.
[9] J. Lin, I. Dahan, B. Valderrama, M. V. Manuel, *Appl. Surf. Sci.* **2014**, *301*, 475–480.
[10] M. M. Strehle, B. J. Heuser, M. S. Elbakhshwan, X. Han, D. J. Gennardo, H. K. Pappas, H. Ju, *Thin Solid Films* **2012**, *520*, 5616–5626.
[11] R. J. McEachern, P. Taylor, *J. Nucl. Mater.* **1998**, *254*, 87–121.
[12] A. K. Burrell, T. M. McCleskey, P. Shukla, H. Wang, T. Durakiewicz, D. P. Moore, C. G. Olson, J. J. Joyce, Q. Jia, *Adv. Mater.* **2007**, *19*, 3559–3563.
[13] B. L. Scott, J. J. Joyce, T. D. Durakiewicz, R. L. Martin, T. M. McCleskey, E. Bauer, H. Luo, Q. Jia, *Coord. Chem. Rev.* **2014**, *266–267*, 137–154.
[14] H. Pierson, *Handbook of Chemical Vapor Deposition (CVD)*, **1999**.
[15] S. T. Barry, *Coord. Chem. Rev.* **2013**, *257*, 3192–3201.
[16] F. T. Edelmann, *Chem. Soc. Rev.* **2012**, *41*, 7649–7964.
[17] B. S. Lim, A. Rahtu, J.-S. Park, R. G. Gordon, *Inorg. Chem.* **2003**, *42*, 7951–7958.
[18] T. B. Thiede, M. Krasnopolski, A. P. Milanov, T. de los Arcos, A. Ney, H.-W. Becker, D. Rogalla, J. Winter, A. Devi, R. A. Fischer, | *Chem. Mater* **2011**, *23*, 1430–1440.
[19] M. Gebhard, M. Hellwig, A. Kroll, D. Rogalla, M. Winter, B. Mallick, A. Ludwig, M. Wiesing, A. D. Wieck, G. Grundmeier, et al., *Dalton Trans.* **2017**, *38*, 819.
[20] R. C. Smith, T. Ma, N. Hoilien, L. Y. Tsung, M. J. Bevan, L. Colombo, J. Roberts, S. A. Campbell, W. L. Gladfelter, *Adv. Mater. Opt. Electron.* **2000**, *10*, 105–114.
[21] Y. Shi, L. Li, *Chem. Soc. Rev.* **2015**, *44*, 2744–2756.
[22] C. H. Winter, P. H. Sheridan, T. S. Lewkebandara, M. J. Heeg, J. W. Proscialc, *J. Am. Chem. Soc.* **1992**, *114*, 1095–1097.
[23] Y. Shiokawa, R. Amano, A. Nomura, M. Yagi, *J. Radioanal. Nucl. Chem.* **1991**, *152*, 373–380.
[24] L. Appel, J. Leduc, C. L. Webster, J. W. Ziller, W. J. Evans, S. Mathur, *Angew. Chem. Int. Ed.* **2015**, *54*, 2209–2213.
[25] M. D. Straub, S. Hohloch, S. G. Minasian, J. Arnold, *Dalton Trans.* **2018**, *47*, 1772–1776.
[26] A. L. Catherall, M. S. Hill, A. L. Johnson, G. Kociok-Köhn, M. F. Mahon, *J. Mater. Chem. C* **2016**, *4*, 10731–10739.
[27] T. Perera, *Wayne State University Dissertation* **2012**.
[28] M. C. Karunarathne, J. W. Baumann, M. J. Heeg, P. D. Martin, C. H. Winter, *J. Organomet. Chem.* **2017**, *847*, 204–212.
[29] C. Li, R. K. Thomson, B. Gillon, B. O. Patrick, L. L. Schafer, *Chem. Commun.* **2003**, *98*, 2462.

10.1002/anie.201901924

WILEY-VCH

Entry for the Table of Contents (Please choose one layout)

Layout 2:

COMMUNICATION

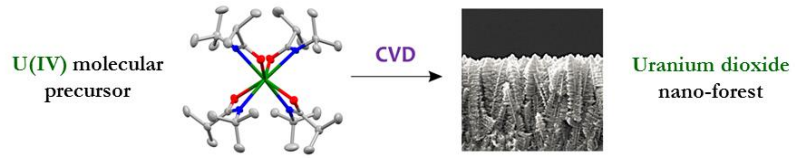

From molecules to materials: Volatile uranium(IV) amidate complexes are used as single-source molecular precursors to uranium oxide films. Chemical vapor deposition (CVD) of these single-source precursors yields crystalline, phase-pure UO_2 films with a fir tree-like microstructure and a high surface area.

M. D. Straub, J. Leduc, M. Frank, A. Raauf, T. D. Lohrey, S. G. Minasian, S. Mathur, and J. Arnold**

Page No. – Page No.

Chemical Vapor Deposition of Phase-Pure Uranium Dioxide Thin Films from Uranium(IV) Amidate Precursors